Geophysical Research Letters

RESEARCH LETTER
10.1029/2018GL077092

Summer Drivers of Atmospheric Variability Affecting Ice Shelf Thinning in the Amundsen Sea Embayment, West Antarctica

Pranab Deb[1,2], Andrew Orr[1], David H. Bromwich[3], Julien P. Nicolas[3], John Turner[1], and J. Scott Hosking[1]

[1]British Antarctic Survey, Cambridge, UK, [2]Now at Climatic Research Unit, School of Environmental Sciences, University of East Anglia, Norwich, UK, [3]Byrd Polar and Climate Research Center, Ohio State University, Columbus, OH, USA

Key Points:
- El Niño episodes during austral summer drive warmer conditions over Amundsen Sea Embayment ice shelves that cause enhanced surface melting
- An eastward shift of the Amundsen Sea Low and positive Southern Annular Mode episodes lead to anomalous westerly winds over the continental shelf edge
- The projected future increase in El Niño episodes and positive trend in the SAM could increase the risk of disintegration of West Antarctic ice shelves

Supporting Information:
- Supporting Information S1

Correspondence to:
P. Deb,
p.deb@uea.ac.uk

Citation:
Deb, P., Orr, A., Bromwich, D. H., Nicolas, J. P., Turner, J., & Hosking, J. S. (2018). Summer drivers of atmospheric variability affecting ice shelf thinning in the Amundsen Sea Embayment, West Antarctica. *Geophysical Research Letters*, *45*, 4124–4133. https://doi.org/10.1029/2018GL077092

Received 9 JAN 2018
Accepted 14 APR 2018
Accepted article online 23 APR 2018
Published online 14 MAY 2018

Abstract Satellite data and a 35-year hindcast of the Amundsen Sea Embayment summer climate using the Weather Research and Forecasting model are used to understand how regional and large-scale atmospheric variability affects thinning of ice shelves in this sector of West Antarctica by melting from above and below (linked to intrusions of warm water caused by anomalous westerlies over the continental shelf edge). El Niño episodes are associated with an increase in surface melt but do not have a statistically significant impact on westerly winds over the continental shelf edge. The location of the Amundsen Sea Low and the polarity of the Southern Annular Mode (SAM) have negligible impact on surface melting, although a positive SAM and eastward shift of the Amundsen Sea Low cause anomalous westerlies over the continental shelf edge. The projected future increase in El Niño episodes and positive SAM could therefore increase the risk of disintegration of West Antarctic ice shelves.

Plain Language Summary Most of the floating ice shelves fringing the Amundsen Sea Embayment (ASE) region of West Antarctica have undergone rapid thinning by basal melting in recent decades, resulting in upstream acceleration of grounded ice and raising global sea levels. Recent climate model projections suggest an intensification of austral summer melt over the ASE ice shelves by the end of the century due to increasing summer air temperatures to magnitudes that caused the recent breakup of ice shelves in Antarctic Peninsula. However, so far, the effect of regional and large-scale atmospheric variability on summertime thinning of ASE ice shelves has not been quantified in a spatially explicit manner. Here we employ a high-resolution regional model and satellite data to show that the location of Amundsen Sea Low, the polarity of Southern Annular Mode, and the phase of El Niño–Southern Oscillation are responsible for pronounced changes in the zonal wind stress over the ASE continental shelf edge and temperatures above the melting point over ASE ice shelves. Particularly, El Niño events are associated with enhanced surface melting over Pine Island and Thwaites Glaciers. The projected future increase in El Niño episodes could therefore increase the risk of disintegration of ASE ice shelves.

1. Introduction

The melting of glacial ice from West Antarctica is of critical concern to vulnerable coastal communities around the world who are at long-term risk from the ensuing global sea level rise. The ice streams draining into the Amundsen Sea (AS) Embayment (ASE) sector of West Antarctica have received much attention recently (Scambos et al., 2017; Turner et al., 2017), as ice discharge has increased by 77% since 1973 due to glacier acceleration and thinning (Mouginot et al., 2014). Pine Island and Thwaites Glaciers are two of the major ice streams flowing into the ASE that are accelerating rapidly (Mouginot et al., 2014). These glaciers and their catchment areas together contain enough ice to raise global sea level by approximately 1.2 m and are currently contributing around 10% of the rate of global sea level rise (Shepherd et al., 2012). Concurrent with these changes is the thinning of the fringing ice shelves, which act to buttress the flow of outlet glacier ice (e.g., Dupont & Alley, 2005; Paolo et al., 2015; Pritchard et al., 2012; Reese et al., 2017).

The recent substantial grounding-line retreat and mass loss of ASE glaciers are/have been driven mainly by melting below the ice shelves due to intrusions of relatively warm circumpolar deep water (CDW) along glacial troughs that cross the AS continental shelf (Jenkins et al., 2016; Payne et al., 2004; Prichard et al., 2012). The rate of delivery of CDW onto the continental shelf is partially controlled by the direction and magnitude of zonal wind stress at the continental shelf edge, with westerly winds causing inflow of CDW onto the shelf (Carvajal et al., 2013; Dutrieux et al., 2014; Jenkins et al., 2016; Thoma et al., 2008). Relatively low-magnitude

surface melting during austral summer (December-January-February) has also been observed across ASE ice shelves (Tedesco, 2009; Trusel et al., 2013). Both Pine Island and Thwaites Glaciers are susceptible to unstable retreat of the grounding line due to the bedrock deepening inland and lying well below sea level (Rignot et al., 2014).

Climate model projections suggest an intensification of summer surface melting over the ASE ice shelves by the end of the century due to increasing air temperatures to magnitudes that caused the recent breakup of ice shelves in the Antarctic Peninsula (Trusel et al., 2015). As the melting of ice shelves from both below and above is strongly controlled (directly or indirectly) by the atmosphere, both processes could potentially work synergistically in the future to increase the risk of catastrophic ice shelf disintegration, followed by the collapse of the West Antarctic ice sheet (DeConto & Pollard, 2016; Reese et al., 2017; Ritz et al., 2015). A clearer understanding of the drivers of interannual atmospheric variability affecting ASE ice shelves in the present-day climate is therefore essential to assess the likelihood of future atmosphere-driven impacts.

Both regional and large-scale climate variability influences the ASE (Scambos et al., 2017; Turner et al., 2017 for a review). The atmospheric circulation in this region is one of the most variable on Earth (Connolley, 1997), largely as a result of variations in the depth and longitudinal location of the Amundsen Sea Low (ASL), which is a climatological low pressure center located off the coast of West Antarctica (Coggins & McDonald, 2015; Hosking et al., 2013; Nicolas & Bromwich, 2011). Although the mean position of the ASL is located over the eastern AS/Bellingshausen Sea during summer, this season corresponds to the largest interannual variability in longitude (Hosking et al., 2013). Important patterns of large-scale variability include the Southern Annular Mode (SAM) and tropical forcing associated with El Niño–Southern Oscillation (ENSO) activity (Clem et al., 2017; Hosking et al., 2013; Nicolas et al., 2017). Note that strong SAM events are able to modulate the ENSO teleconnection (Fogt & Bromwich, 2006).

In recent decades, the SAM has shifted toward its positive polarity in summer largely because of the Antarctic ozone hole (Polvani, Previdi, & Deser, 2011). Continued increased emissions of greenhouse gases is likely to keep it more often in its positive polarity throughout the 21st century, despite the anticipated Antarctic ozone recovery partially offsetting this (Polvani, Waugh, et al., 2011). Climate model projections also suggest that the mean position of the ASL during summer under the Representative Concentration Pathway experiment 8.5 emissions scenario will shift westward toward the AS by the end of the 21st century (Hosking et al., 2016). Modeling experiments additionally suggest a trend toward stronger and more frequent El Niño episodes during the 21st century (e.g., Cai et al., 2014; Power et al., 2013), along with an increase in ENSO interannual variability (e.g., X.-T. Zheng et al., 2016).

The aim of this study is to demonstrate the influence of these drivers on ice shelf melt processes in the ASE during summer. Our results will enable better prediction of how the glaciers draining into the ASE will evolve over the coming decades and the possible impact on sea levels.

2. Materials and Methods

Although global atmospheric reanalysis products have been used previously to characterize the present-day climate of the ASE (Jones et al., 2016), they are unable to resolve the relatively narrow ASE ice shelves (~50-km width) due to their coarse grid spacing of 50–100 km. Moreover, due to the remoteness of the region, there are no long-term in situ meteorological records. We overcame both of these deficiencies by producing a 35-year high-resolution hindcast for this region using an atmosphere-only model to dynamically downscale the reanalysis data to a grid spacing of 15 km, which, as shown by Deb et al. (2016), has comparable skill to model output at 5-km spacing at coastal ASE sites.

The model uses the recommended configuration of version 3.5.1 of the polar modified Weather Research and Forecasting model (known as "Polar WRF"; Bromwich et al., 2013) for the ASE described by Deb et al. (2016), which realistically simulated the near-surface meteorological conditions over coastal sites during summer. The physics selections include the WRF Single Moment 5-Class cloud microphysics scheme, the Mellor-Yamada-Janjic boundary layer scheme, the Rapid Radiative Transfer Model for General Circulation Models, and the Noah land surface model. The model outer domain encompasses the West Antarctic ice sheet and a large part of the surrounding ocean at 45-km horizontal grid spacing, and the nested (one-way) inner domain covers the ASE at 15-km grid spacing (see Figure 1a). Both domains have a model top of 50 hPa

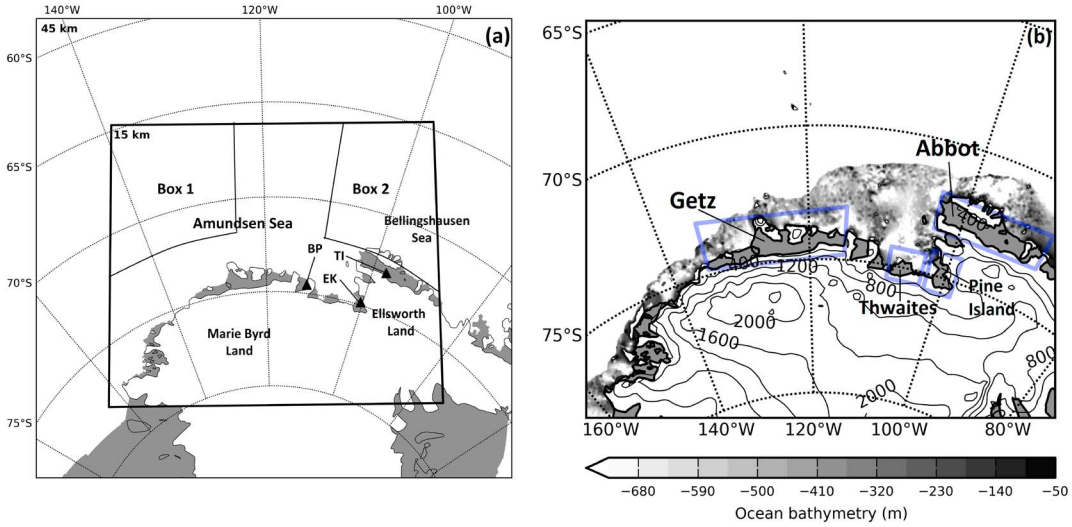

Figure 1. Map showing the model domain setup of the hindcast simulations. (a) The 45-km outer domain and the 15-km inner nested domain, as well as the two sectors used to compute the "ASL-Ion" index (indicated by the regions labeled "Box 1" and "Box 2"), the locations of the Amundsen Sea, Bellingshausen Sea, Marie Byrd Land, Ellsworth Land, ice shelves (shaded in gray), and the coastal AWSs (solid black triangles) at Bear Peninsula (BP), Evans Knoll (EK), and Thurston Island (TI). (b) Zoom in of the 15-km inner nested domain showing the locations of the Getz, Thwaites, Pine Island and Abbot Ice Shelves (shaded in gray and enclosed by magenta boxes), the model topographic height based on the Bedmap2 data set (solid gray contours), and the ocean bathymetry based on the ETOPO1 data set (gray shading over the ocean, m).

and 30 vertical levels. Also used are spectral nudging (outer domain and wave numbers 1–5 only, from approximately 1.5 km to the model top), high-resolution orography based on the Bedmap2 data set, and meteorological forcing from ERA-Interim reanalysis (Dee et al., 2011). Additionally, the surface boundary forcing of the model includes daily satellite observations of sea ice concentration (based on the 25-km resolution Bootstrap data set; Comiso, 2000) and sea surface temperature (based on the 0.25° Advanced Very High Resolution Radiometer data set; Casey et al., 2010). Only model output at 15-km grid spacing and hourly temporal resolution is analyzed in this study.

The hindcast was produced by running separate simulations for each of the summer months from December 1979 to February 2015 (with 24-hr spin up). Note that the monthly model output in this study is based on a 30-day model month for December and January and a 28-day model month for February (ending at 18 UTC of the last day of each month). Along with Pine Island and Thwaites, a focus of this study is the Abbot and Getz Ice Shelves (see Figure 1b for locations), which are selected both because of their relatively large areas and to distinguish the impacts at different locations of the ASE, although Getz does show evidence of grounding line retreat (Chuter et al., 2017). Note that Figure 1b additionally shows the bathymetry of the continental shelf, based on the ETOPO1 data set (Amante & Eakins, 2009). The model representation of meteorological variables for each of the ice shelves is computed by averaging over all grid points within the boxes enclosing them (see Figure 1b), excluding any ocean points.

Monthly temperature data from three coastal automatic weather stations (AWSs) at Bear Peninsula, Evans Knoll, and Thurston Island (length of summer temperature records of 14, 11, and 8 months, respectively) were collected to further assess the model representation temperature at 2 m (see Figure 1b for their locations). No adjustment was made to account for the difference between the height of the AWS measurements (3 m) and that of the model temperature. A statistical comparison between the monthly averaged model temperature at 2 m and the monthly temperature records from the three AWSs demonstrated a significant correlation ranging from 0.95 to 0.98, a bias ranging from around −0.02 to −1.04°C, and a root mean square error ranging from 0.66 to 1.14°C (see supporting information Table S1 for details). These results confirm the findings of Deb et al. (2016) that the setup of the Polar WRF deployed for this study is able to represent realistically summertime near-surface temperatures in the coastal ASE region.

In our hindcast, meltwater volume is simulated by the WRF Noah land surface model. Modeled melt days are defined as days with cumulated meltwater volume >3 mm (note that the same value was also used by

Lenaerts et al., 2017, with the RACMO2 regional model). The model results are compared with the number of melt days estimated from satellite passive microwave measurements and defined as days with at least one occurrence of surface melt. The satellite data have a grid spacing of 25 km and cover the same period as the hindcast simulations. See Nicolas et al. (2017) for further details about the data and the algorithm used to convert brightness temperatures into melted/nonmelted grid points.

We defined an index based on the differences between summer mean sea level pressure averaged over a box in the western AS region (to the west of 125°W; labeled "Box 1" in Figure 1a) and a box in the Bellingshausen Sea (to the east of 110°W, labeled "Box 2"). The index (referred to as "ASL-lon" hereafter) represents a westward (eastward) shift of the location of the ASL for negative (positive) values. In order to demonstrate the influence of the longitudinal position of the ASL on the ice shelves, composites are constructed by dividing the monthly model output into quartiles based on the ASL-lon index and examining the differences between the lower and upper quartiles (containing 22 and 20 months, respectively), that is, westward minus eastward location of the ASL. Similarly, to demonstrate the influence of the polarity of the SAM, the monthly model output was divided into quartiles based on the SAM index, and the differences between the upper and lower quartiles (containing 18 and 21 months, respectively) were examined, that is, positive SAM minus negative SAM events. The SAM polarity was identified using the Marshal index (Marshall & National Center for Atmospheric Research Staff, 2016). Note that to reduce any signal related to ENSO from the analysis, months with strong ENSO variability are excluded, which are identified by sea surface temperature anomalies above (below) a threshold of +1.5°C (−1.5°C) in the Niño 3.4 region, computed from the HadISST1 data set (Rayner et al., 2003). Finally, to investigate the influence of ENSO, differences are presented for El Niño minus La Niña composites (containing 33 and 38 months, respectively), with El Niño (La Niña) episodes identified from sea surface temperature anomalies above (below) the threshold of +0.5°C (−0.5°C) in the Niño 3.4 region. El Niño and La Niña are opposite phases of ENSO.

3. Results

The composite differences in Figure 2 for westward minus eastward location of the ASL (upper panels) show a marked zonal gradient in surface pressure, with lower pressures (exceeding −5 hPa) over the western AS and higher pressures (exceeding 5 hPa) over the eastern AS/western Bellingshausen Sea. The pressure gradient is linked to a marked strengthening of the meridional wind component at 10 m over the Southern Pacific Ocean (by up to 4 m/s), resulting in an increase in the advection of warm maritime air toward West Antarctica. The flow divides in the horizontal plane as it approaches the continent, with some flowing over the Marie Byrd Land sector of West Antarctica. However, the majority deflects to the right and flows westward over the western AS continental shelf edge due to a combination of the change in pressure gradient and low-level blocking by the coastal orography (cf. Orr et al., 2004), that is, consistent with causing a reduction of warm CDW onto the shelf near Getz. Supporting information Figure S1 shows that a westward (eastward) location of the ASL is associated with, for example, an increase in the frequency of easterly (westerly) wind events over the western Getz continental shelf break. Associated with the wind changes is an increase in temperature at 2 m over West Antarctica, with the Getz Ice Shelf showing the largest warming (of around 1.8 K) of all the ice shelves; although the strongest warming (of around 3 K) occurs over the continental interior (west of around 110°W).

The composite differences for El Niño minus La Niña episodes in Figure 2 (middle panels) show a high-pressure ridge over the AS (exceeding 4 hPa), which strengthens the westerly component of the wind over the continental shelf edge, that is, consistent with causing an increase of warm CDW onto regions of the continental shelf that include Pine Island, Thwaites, and Getz. However, the differences in wind over the continental shelf are weak (less than 1 m/s), as well as not statistically significant. Supporting information Figure S1 confirms that El Niño episodes are associated with only a small increase (decrease) in westerly (easterly) wind events over the eastern Getz continental shelf break, suggesting that the actual influence on CDW upwelling is only marginal. Note that the differences in surface pressure (although prominent) are also not statistically significant, which highlights the large variability associated with ENSO. The enhanced flow transports relatively warm maritime air over the Getz, Pine Island, and Thwaites Ice Shelves and extends deep into the Ellsworth Land sector of West Antarctica (Figure 2f). This accounts for the increases in temperature at 2 m over these regions, with Thwaites and Pine

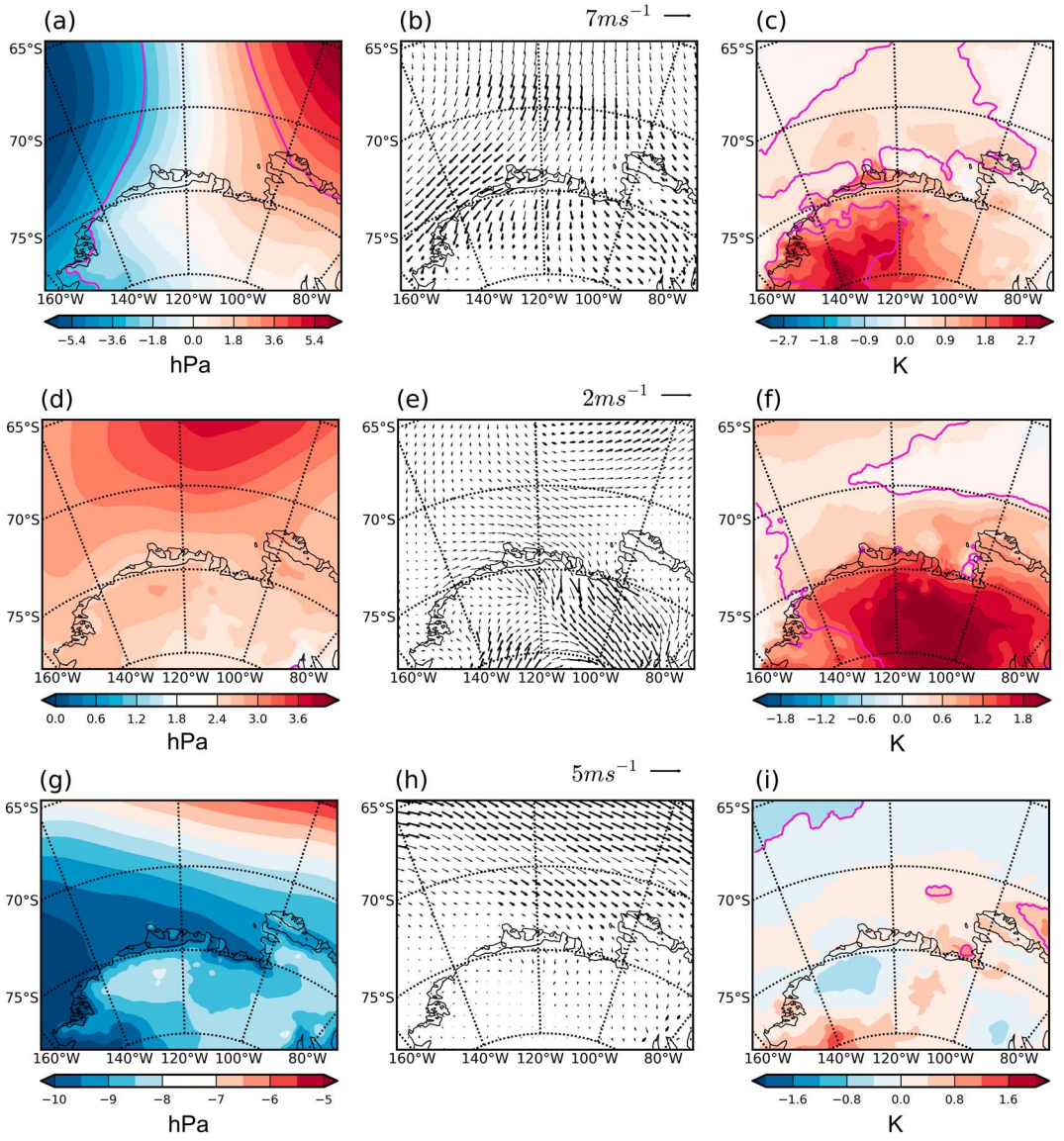

Figure 2. Composite differences for austral summer of (a, d, and g) surface pressure (hPa), (b, e, and h) wind vectors at 10 m (m/s), and (c, f, and i) temperature at 2 m (K) from the hindcast simulations. The upper panels (a–c) show results for westward minus eastward location of Amundsen Sea Low. The middle panels (d–f) show results for El Niño minus La Niña episodes. The lower panels (g–i) show Southern Annular Mode (SAM) positive minus SAM negative events. Solid magenta contours and bold arrows show 90% significance level. Note that the maximum and minimum values of the color bars vary, as do the reference wind arrows. The results for the Amundsen Sea Low location and SAM polarity exclude months with strong ENSO variability.

Island showing the largest warming of all the ice shelves; however, the strongest warming (of around 2 K) again occurs over the continental interior.

As expected, analogous results for composite differences for SAM positive minus SAM negative events in Figure 2 (bottom panels) show a marked meridional gradient in surface pressure. This is associated with strengthened northwesterly winds over the continental shelf edge that includes Pine Island, Thwaites, and Abbot Ice Shelves, that is, associated with increased intrusions of CDW onto the continental shelf. Supporting information Figure S1 shows that positive SAM events are associated with a noticeable reduction in easterly wind events over the Pine Island continental shelf break compared to negative SAM events but only a small increase in westerly wind events. Differences in wind speed and temperature over the ice

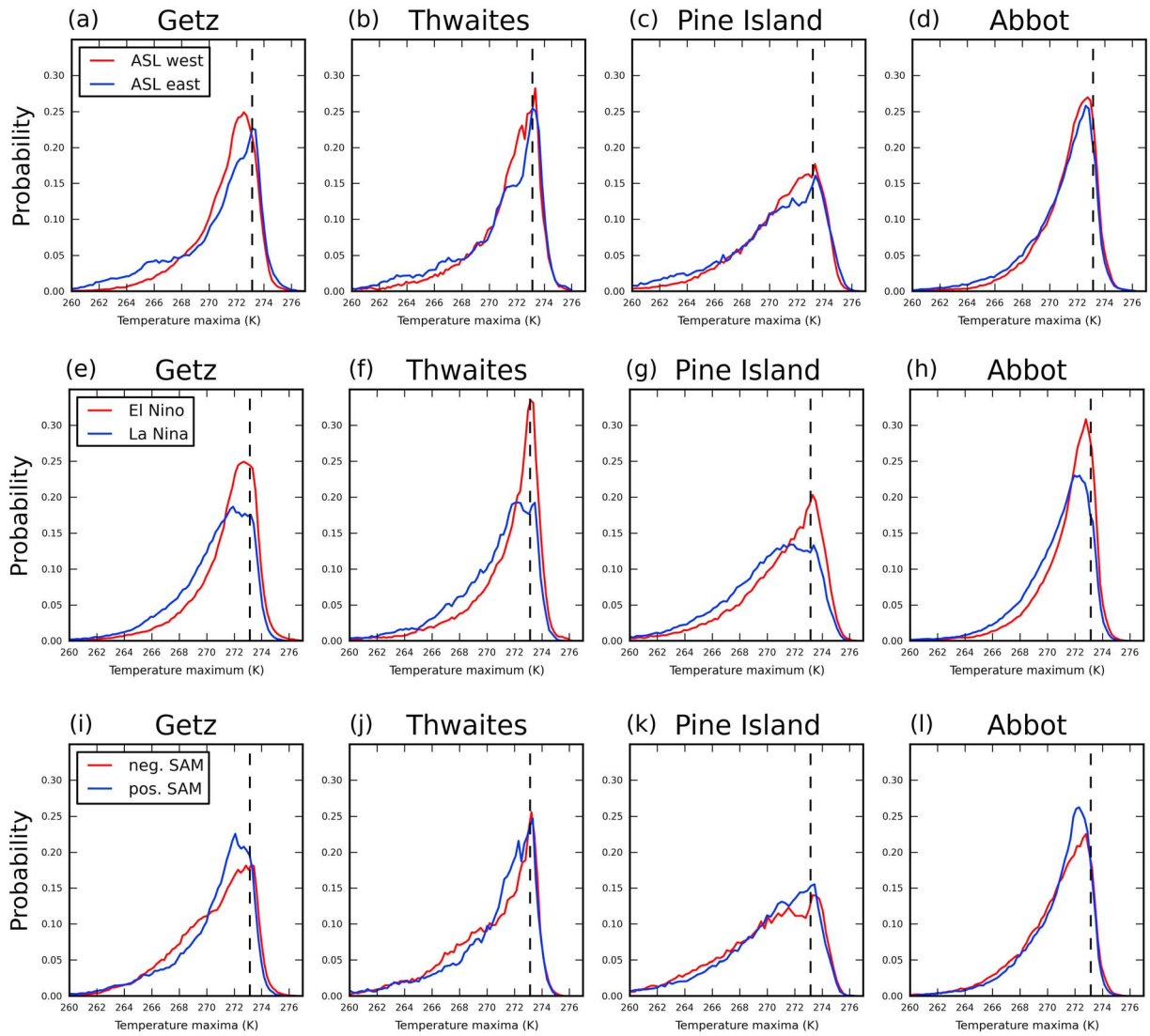

Figure 3. Normalized probability distributions for austral summer of daily maximum temperature at 2 m for (a, e, and i) Getz, (b, f, and j) Thwaites, (c, g, and k) Pine Island, and (d, h, and l) Abbot Ice Shelves from the hindcast simulations. The upper panels (a–d) show results for the ASL located westward in Box 1 (solid red lines) and eastward in Box 2 (solid blue lines). The middle panels (e–h) show results for El Niño (solid red lines) and La Niña (solid blue lines) episodes, for all months. The lower panels (i–l) show results for SAM positive (solid blue lines) and SAM negative (solid red lines) events. The dashed line identifies the melting point (273.15 K). The results for the ASL location and SAM polarity exclude months with strong El Niño–Southern Oscillation variability. ASL = Amundsen Sea Low; SAM = Southern Annular Mode.

shelves and continental interior are small and statistically insignificant, with the exception of a region of isolated warming around Pine Island.

To investigate the impact on temperature extremes, Figure 3 shows the normalized probability distributions of model daily maximum temperature at 2 m for each of the composites. The probability distributions for both westward and eastward locations of the ASL (upper panels) are strongly negatively skewed, with the highest peaks occurring between 272 and 273 K (with a probability of up to 25%). However, the impact of ASL location on maximum temperatures above the melting point is minimal. Nevertheless, compared to an eastward location of the ASL, a westward location broadly causes a decreased frequency in the occurrence of temperatures in the range 260 to 268 K over the ice shelves, coupled with an increase in the range 268 to 273 K. This relationship is most apparent for the Getz Ice Shelf (to the west) and least apparent for the Abbot Ice Shelf (to the east; cf. Figure 2c).

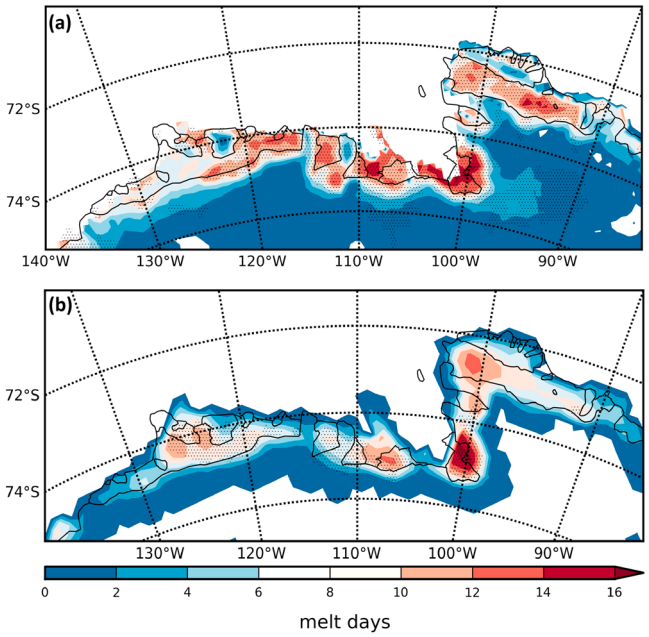

Figure 4. Composite differences for austral summer of the cumulative number of melt days (a) from the hindcast simulations and (b) measured by satellite for El Niño minus La Niña episodes. Hatching shows regions with 90% significance level.

The probability distributions for both the El Niño and La Niña composites are also strongly negatively skewed, with the highest peaks occurring around 273 K (Figure 3, middle panels). However, the distributions for El Niño conditions are shifted to the right compared to La Niña, resulting in an increased probability of the maximum temperature exceeding the melting point. This shift is particularly apparent for the left-hand side tail, resulting in an increase in skewness and a reduction in the spread by up to 2 K. Moreover, El Niño episodes cause a large increase in the highest peaks compared to La Niña episodes, with the likelihood of the maximum temperature occurring around 273 K increasing by up to 75% (Thwaites Ice Shelf). Analogous results for the SAM composites (Figure 3, bottom panels) show that although positive SAM events are broadly associated with an increased frequency of temperatures in the range 270 to 273 K compared to negative SAM events, the impact on temperatures above the melting point are minimal.

To clarify further the role of ENSO in controlling surface melt over the coastal ASE sector, Figure 4 presents composite differences for El Niño minus La Niña episodes for the average number of melt days per summer derived from the model simulations (upper panel) and passive microwave satellite observations (bottom panel). Note that only the sensitivity to ENSO is investigated as temperatures above the melt threshold were relatively insensitive to the polarity of the SAM and longitudinal position of the ASL (Figure 3). Both model- and satellite-based composite differences show a consistent pattern of longer melt duration along the ASE coast during El Niños compared to La Niñas. These results are consistent with the warmer conditions over the entire region favored by El Niños (Figure 2f) and the greater probability of temperatures reaching 0°C under such conditions (Figure 3, middle panels). Some differences between Figures 4a and 4b can be ascribed to factors such as differences in horizontal resolution, temporal frequency, or liquid water detection/simulation thresholds between model- and satellite-based estimates. Nonetheless, in both panels, the increase is most marked over the Pine Island Ice Shelf, with an additional 14 days or more of melting conditions in this area under El Niño conditions. The increase is statistically significant over the Getz, Pine Island, and Thwaites Ice Shelves in both model and satellite results but is only statistically significant over the Abbot Ice Shelf in the model data. Note that examination of individual years showed that not all El Niño episodes resulted in surface melt (not shown).

Ice shelf surface melt is also influenced by precipitation, for example, via the accumulation of a layer of snow that shields the underlying ice surface or rainfalling instead of snow. Results from the hindcast simulations show that a westward shift of the ASL is associated with a widespread increase in precipitation over the coastal sector of the ASE, but there is little sensitivity to ENSO or the polarity of the SAM (supporting information Figure S2). These model results do not take into account the phase of precipitation, for which further investigations are required.

4. Discussion and Conclusions

Many ASE ice shelves have experienced significant basal thinning over recent decades, potentially making them susceptible to a higher risk of collapse due to increased surface melting in a warming climate. The climate of the ASE is strongly influenced by both local and large-scale variability, and a detailed understanding of the effects of this variability on ice shelf melt processes is vital for assessing the likelihood of their future disintegration. A configuration of Polar WRF optimized for the coastal ASE sector is used to investigate this by producing a 35-year hindcast austral summer simulation at a sufficiently detailed resolution to capture the local characteristics of the ice shelves and continental shelf edge.

The hindcast showed that temperatures above the melting point over ASE ice shelves are largely insensitive to either the longitudinal location of the ASL or the polarity of the SAM, in both cases therefore having little impact on surface melting. However, both of these drivers are responsible for pronounced changes in the

zonal wind stress over the ASE continental shelf edge, which influences ice shelf stability by controlling whether CDW can flow onto the continental shelf and reach the glaciers via glacial troughs (Carvajal et al., 2013; Dutrieux et al., 2014; Jenkins et al., 2016; Thoma et al., 2008). An eastward shift of the ASL causes anomalous westerly winds over the continental shelf edge near Getz Ice Shelf, while positive SAM episodes cause anomalous westerly winds over the sectors of the continental shelf edge that includes Pine Island, Thwaites, and Abbot Ice Shelves, increasing the flow of warm CDW onto these regions of the continental shelf.

By contrast, the occurrence of El Niño episodes causes a sharp increase in the likelihood of temperatures exceeding the melting point, which is reflected in a substantial increase in surface melt over the ice shelves, especially for Pine Island and Thwaites Ice Shelves. The importance of El Niño to the meteorology of the West Antarctic Ice Sheet is further evidenced by its role in the 2016 widespread and prolonged melt over the Ross Ice Shelf (Nicolas et al., 2017). However, El Niño episodes have only a small and statistically nonsignificant impact on westerly winds over the continental shelf edge compared to La Niña episodes. It is worth noting that we have described the impact of ENSO variability in summer on summer atmospheric anomalies in the ASE region; however, the findings from Clem et al. (2017) suggest that the latter could also be influenced by ENSO variability in spring. It is further worth noting that the modulation of the influence of ENSO by SAM is a major reason for why not all El Niño episodes result in surface melt over the ice shelves; for example, the high-latitude ENSO teleconnection is reduced in El Niño/positive SAM combinations (Fogt & Bromwich, 2006). Other factors to consider are the timing of the ENSO variability during summer, as well as changes in the location of the ENSO teleconnection pattern in the South Pacific (e.g., Wilson et al., 2016).

Model experiments suggest a higher frequency of positive SAM conditions by the end of the 21st century due to climate change (e.g., F. Zheng et al., 2013), which would be conducive to increased basal-driven melting of ASE ice shelves. Although limitations in climate models make projected changes in ENSO and associated teleconnections to the ASE uncertain (Bracegirdle et al., 2014), such model experiments also suggest a trend toward stronger and more frequent El Niño episodes during the 21st century, which would result in increased surface melting of ASE ice shelves. Although projections also suggest that the mean position of the ASL under Representative Concentration Pathway experiment 8.5 during summer will shift westward by the end of the 21st century (Hosking et al., 2016), the shift is much smaller than the longitudinal differences considered here.

Our study suggests that ASE ice shelves could experience an intensification of melt in the future from both above and below as a result of both regional and large-scale atmospheric changes, potentially increasing the risk of their disintegration, which in turn could potentially trigger a collapse of the West Antarctic ice sheet (DeConto & Pollard, 2016). To better understand this threat will require further detailed investigation of the impacts of ENSO, the polarity of the SAM, and the depth/location of the ASL on ASE ice shelves. Also necessary is improving the reliability of future projections, such as ENSO and its teleconnections, as well as the response of the SAM to recovery of the Antarctic ozone hole and increased greenhouse gas emissions (Polvani, Waugh, et al., 2011).

Acknowledgments
The authors would like to thank Tom Bracegirdle, Paul Holland, Adrian Jenkins (British Antarctic Survey), Kyle Clem (Rutgers University), and Tony Payne (University of Bristol) for useful conversations, as well as the two anonymous reviewers for their insightful comments that helped to considerably improve this study. The AWS data were obtained from the University of Wisconsin-Madison Automatic Weather Station Program, with special thanks to Matthew Lazzara. The satellite-based melt data are based on passive microwave satellite data obtained from the National Snow and Ice Data Center. Both the satellite-based melt data (https://doi.org/10.5285/ffd24dd7-e201-4a02-923f-038680bf7bb5) and the Polar WRF hindcast data (https://doi.org/10.5285/9536f22e-37dd-4f37-948b-e19c70e15292) used in this study are archived at the UK Polar Data Centre (based at British Antarctic Survey), with special thanks to Tony Phillips for his assistance. The Natural Environment Research Council (NERC) under grant NE/K00445X/1 and the National Science Foundation under grants PLR 134165 and PLR 1443443 supported this study. This is contribution 1575 of the Byrd Polar and Climate Research Center.

References

Amante, C., & Eakins, B. W. (2009). ETOPO1 arc-minute global relief model: Procedures, data sources and analysis, NOAA Technical Memorandum, NESDIS NGDC-24.

Bracegirdle, T. J., Turner, J., Hosking, J. S., & Phillips, T. (2014). Sources of uncertainty in projections of twenty-first century westerly wind changes over the Amundsen Sea, West Antarctica, in CMIP5 climate models. *Climate Dynamics*, *43*(7-8), 2093–2104. https://doi.org/10.1007/s00382-013-2032-1

Bromwich, D. H., Otieno, F. O., Hines, K. M., Manning, K. W., & Shilo, E. (2013). Comprehensive evaluation of polar weather research and forecasting performance in the Antarctic. *Journal of Geophysical Research: Atmospheres*, *118*, 274–292. https://doi.org/10.1029/2012JD018139

Cai, W., Borlace, S., Lengaigne, M., van Rensch, P., Collins, M., Vecchi, G., et al. (2014). Increasing frequency of extreme El Niño events due to greenhouse warming. *Nature Climate Change*, *4*(2), 111–116. https://doi.org/10.1038/nclimate2100

Carvajal, G. K., Wåhlin, A. K., Eriksson, L. E. B., & Ulander, L. M. H. (2013). Correlation between synthetic aperture radar surface winds and deep water velocity in the Amundsen Sea, Antarctica. *Remote Sensing*, *5*(8), 4088–4106. https://doi.org/10.3390/rs5084088

Casey, K., Brandon, T., Cornillion, P., & Evans, R. (2010). The past, present, and future of the AVHRR pathfinder SST program. In V. Barale, J. Gower, & L. Alberotanza (Eds.), *Oceanography from space: Revisited* (pp. 273–287). Netherlands: Springer. https://doi.org/10.1007/978-90-481-8681-5_16

Chuter, S. J., Martin-Espanol, A., Wouters, B., & Bamber, J. L. (2017). Mass balance reassessment of glaciers draining into the Abbot and Getz ice shelves in West Antarctica. *Geophysical Research Letters*, *44*, 7328–7337. https://doi.org/10.1002/2017GL073087

Clem, K. R., Renwick, J. A., & McGregor, J. (2017). Large-scale forcing of the Amundsen Sea Low and its influence on sea ice and West Antarctic temperature. *Journal of Climate*, *30*(20), 8405–8424. https://doi.org/10.1175/JCLI-D-16-0891.1

Coggins, J. H. G., & McDonald, A. (2015). The influence of the Amundsen Sea Low on the winds in the Ross Sea and surroundings: Insights from a synoptic climatology. *Journal of Geophysical Research: Atmospheres*, *120*, 2167–2189. https://doi.org/10.1002/2014JD022830

Comiso, J. C. (2000). Bootstrap sea ice concentrations from NIMBUS-7 SMMR and DMSP SSM/I-SSM/S, version 2, subset used: December, January, February from 1979 to 2015, NASA DAAC at the National Snow and Ice Data Center, Boulder, Colorado.

Connolley, W. M. (1997). Variability in annual mean circulation in southern high latitudes. *Climate Dynamics*, *13*, 745–756. https://doi.org/10.1007/s003820050195

Deb, P., Orr, A., Hosking, J. S., Phillips, T., Turner, J., Bannister, D., et al. (2016). An assessment of the Polar Weather Research and Forecasting (WRF) model representation of near-surface meteorological variables over West Antarctica. *Journal of Geophysical Research: Atmospheres*, *121*, 1532–1548. https://doi.org/10.1002/2015JD024037

DeConto, R. M., & Pollard, D. (2016). Contribution of Antarctica to past and future sea-level rise. *Nature*, *531*(7596), 591–597. https://doi.org/10.1038/nature17145

Dee, D. P., Uppala, S. M., Simmons, A. J., Berrisford, P., Poli, P., Kobayashi, S., et al. (2011). The ERA-interim reanalysis: Configuration and performance of the data assimilation system. *Quarterly Journal of the Royal Meteorological Society*, *137*(656), 553–597. https://doi.org/10.1002/qj.828

Dupont, T. K., & Alley, R. B. (2005). Assessment of the importance of ice-shelf buttressing to ice-sheet flow. *Geophysical Research Letters*, *32*, L04503. https://doi.org/10.1029/2004GL022024

Dutrieux, P., De Rydt, J., Jenkins, A., Holland, P. R., Kyung Ha, H., Hoon Lee, S., et al. (2014). Strong sensitivity of Pine Island ice-shelf melting to climatic variability. *Science*, *343*(6167), 174–178. https://doi.org/10.1126/science.1244341

Fogt, R. L., & Bromwich, D. H. (2006). Decadal variability of the ENSO teleconnection to the high latitude South Pacific governed by coupling with the Southern Annular Mode. *Journal of Climate*, *19*(6), 979–997. https://doi.org/10.1175/JCLI3671.1

Hosking, J. S., Orr, A., Bracegirdle, T. J., & Turner, J. (2016). Future circulation changes off West Antarctica: Sensitivity of the Amundsen Sea Low to projected anthropogenic forcing. *Geophysical Research Letters*, *43*, 367–376. https://doi.org/10.1002/2015GL067143

Hosking, J. S., Orr, A., Marshall, G. J., Turner, J., & Phillips, T. (2013). The influence of the Amundsen-Bellingshausen Seas Low on the climate of West Antarctica and its representation in coupled climate model simulations. *Journal of Climate*, *26*(17), 6633–6648. https://doi.org/10.1175/JCLI-D-12-00813.1

Jenkins, A., Dutrieux, P., Jacobs, S., Steig, E. J., Gudmundsson, G. H., Smith, J., & Heywood, K. J. (2016). Decadal ocean forcing and Antarctic ice sheet response: Lessons from the Amundsen Sea. *Oceanography*, *29*(4), 106–117. https://doi.org/10.5670/oceanog.2016.103

Jones, R. W., Renfrew, I. A., Orr, A., Webber, B. G. M., Holland, D. M., & Lazzara, M. A. (2016). Evaluation of four reanalysis products using in situ observations in the Amundsen Sea Embayment, Antarctica. *Journal of Geophysical Research: Atmospheres*, *121*, 6240–6257. https://doi.org/10.1002/2015JD024680

Lenaerts, J., Ligtenberg, S., Medley, B., Van de Berg, W., Konrad, H., Nicolas, J. P., et al. (2017). Climate and surface mass balance of coastal West Antarctica resolved by regional climate modelling. *Annals of Glaciology*, 1–13. https://doi.org/10.1017/aog.2017.42

Marshall, G., & National Center for Atmospheric Research Staff (Eds.) (2016). Last modified 10 Jun 2016. "The climate data guide: Marshall Southern Annular Mode (SAM) index (station-based)". Retrieved from https://climatedataguide.ucar.edu/climate-data/marshall-southern-annular-mode-sam-index-station-based

Mouginot, J., Rignot, E., & Scheuchl, B. (2014). Sustained increase in ice discharge from the Amundsen Sea Embayment, West Antarctica, from 1973 to 2013. *Geophysical Research Letters*, *41*(5), 1576–1584. https://doi.org/10.1002/2013GL059069

Nicolas, J. P., & Bromwich, D. H. (2011). Climate of West Antarctica and influence of marine air intrusions. *Journal of Climate*, *24*(1), 49–67. https://doi.org/10.1175/2010JCLI3522.1

Nicolas, J. P., Vogelmann, A. M., Scott, R. C., Wilson, A. B., Cadeddu, M. P., Bromwich, D. H., et al. (2017). January 2016 extensive summer melt in West Antarctica favoured by strong El Niño. *Nature Communications*, *8*, 15799. https://doi.org/10.1038/ncomms15799

Orr, A., Cresswell, D., Marshall, G. J., Hunt, J. C. R., Sommeria, J., Wang, C. G., & Light, M. (2004). A 'low-level' explanation for the recent large warming trend over the western Antarctic Peninsula involving blocked winds and changes in zonal circulation. *Geophysical Research Letters*, *31*, L06204. https://doi.org/10.1029/2003GL019160

Paolo, F. S., Fricker, H. A., & Padman, L. (2015). Volume loss from Antarctic ice shelves is accelerating. *Science*, *348*(6232), 327–331. https://doi.org/10.1126/science.aaa0940

Payne, A. J., Vieli, A., Shepherd, A. P., Wingham, D. J., & Rignot, E. (2004). Recent dramatic triggering of largest West Antarctic ice stream triggered by oceans. *Geophysical Research Letters*, *31*, L23401. https://doi.org/10.1029/2004GL021284

Polvani, L. M., Previdi, M., & Deser, C. (2011). Large cancellation, due to ozone recovery, of future Southern Hemisphere atmospheric circulation trends. *Geophysical Research Letters*, *38*, L04707. https://doi.org/10.1029/2011GL046712

Polvani, L. M., Waugh, D. W., Correa, G. J. P., & Son, S.-W. (2011). Stratospheric ozone depletion: The main driver of 20th century atmospheric changes in the Southern Hemisphere. *Journal of Climate*, *24*(3), 795–812. https://doi.org/10.1175/2010JCLI3772.1

Power, S., Delage, F., Chung, C., Kociuba, G., & Keay, K. (2013). Robust twenty-first-century projections of El Niño and related precipitation variability. *Nature*, *502*(7472), 541–545. https://doi.org/10.1038/nature12580

Pritchard, H. D., Ligtenberg, S. R. M., Fricker, H. A., Vaughan, D. G., van den Broeke, M. R., & Padman, L. (2012). Antarctic ice-sheet loss driven by basal melting of ice shelves. *Nature*, *484*(7395), 502–505. https://doi.org/10.1038/nature10968

Rayner, N. A., Parker, D. E., Horton, E. B., Folland, C. K., Alexander, L. V., Rowell, D. P., et al. (2003). Global analyses of sea surface temperature, sea ice, and night marine air temperature since the late nineteenth century. *Journal of Geophysical Research*, *108*(D14), 4407. https://doi.org/10.1029/2002JD002670

Reese, R., Gudmundsson, G. H., Levermann, A., & Winklemann, R. (2017). The far reach of ice-shelf thinning in Antarctica. *Nature Climate Change*, *8*(1), 53–57. https://doi.org/10.1038/s41558-017-0020-x

Rignot, E., Mouginot, J., Morlighen, M., Seroussi, H., & Scheuchl, B. (2014). Widespread, rapid grounding line retreat of Pine Island, Thwaites, Smith, and Kohler glaciers, West Antarctica, from 1992 to 2011. *Geophysical Research Letters*, *41*(10), 3502–3509. https://doi.org/10.1002/2014GL060140

Ritz, C., Edwards, T. L., Durand, G., Payne, A. J., Peyaud, V., & Hindmarsh, R. C. A. (2015). Potential sea-level rise from Antarctic ice-sheet instability constrained by observations. *Nature*, *528*, 115–118. https://doi.org/10.1038/nature16147

Scambos, T. A., Bell, R. E., Alley, R. B., Anandakrishnan, S., Bromwich, D. H., Brunt, K., et al. (2017). How much, how fast?: A science review and outlook for research on the instability of Antarctica's Thwaites Glacier in the 21st century. *Global and Planetary Change*, *153*, 16–34. https://doi.org/10.1016/j.gloplacha.2017.04.008

Shepherd, A., Ivins, E. R., Geruo, A., Barletta, V. R., Bentley, M. J., Bettadpur, S., & Briggs, K. H. (2012). A reconciled estimate of ice-sheet mass balance. *Science*, *338*(6111), 1183–1189. https://doi.org/10.1126/science.1228102

Tedesco, M. (2009). Assessment and development of snowmelt retrieval algorithms over Antarctica from K-band spaceborne brightness temperature (1979–2008). *Remote Sensing of Environment*, *113*(5), 979–997. https://doi.org/10.1016/j.rse.2009.01.009

Thoma, M., Jenkins, A., Holland, D., & Jacobs, S. (2008). Circumpolar intrusions on the Amundsen Sea continental shelf, Antarctica. *Geophysical Research Letters*, *35*, L18602. https://doi.org/10.1029/2008GL034939

Trusel, L. D., Frey, K. E., Das, S. B., Karnauskas, K. B., Kuipers Munneke, P., van Meijgaard, E., & van den Broeke, M. R. (2015). Divergent trajectories of Antarctic surface melt under two twenty-first-century climate scenarios. *Nature Geoscience*, *8*(12), 927–932. https://doi.org/10.1038/ngeo2563

Trusel, L. D., Frey, K. E., Das, S. B., Kuipers Munneke, P., & van den Broeke, M. R. (2013). Satellite-based estimates of Antarctic surface meltwater fluxes. *Geophysical Research Letters*, *40*, 6148–6153. https://doi.org/10.1002/2013GL058138

Turner, J., Orr, A., Gudmundsson, G. H., Jenkins, A., Bingham, R. G., Hillenbrand, C.-D., & Bracegirdle, T. J. (2017). Atmosphere-ocean-ice interactions in the Amundsen Sea Embayment, West Antarctica. *Reviews of Geophysics*, *55*, 235–276. https://doi.org/10.1002/2016RG000532

Wilson, A. B., Bromwich, D. H., & Hines, K. M. (2016). Simulating the mutual forcing of anomalous high-southern latitude atmospheric circulation by El Niño flavours and the Southern Annular Mode. *Journal of Climate*, *29*(6), 2291–2309. https://doi.org/10.1175/JCLI-D-15-0361.1

Zheng, F., Li, J., Clark, R. T., & Nnamchi, H. C. (2013). Simulation and projection of the Southern Hemisphere annular mode in CMIP5 models. *Journal of Climate*, *26*(24), 9860–9879. https://doi.org/10.1175/JCLI-D-13-00204.1

Zheng, X.-T., Xie, S.-P., Lv, L.-H., & Zhou, Z.-Q. (2016). Intermodel uncertainty in ENSO amplitude change tied to Pacific Ocean warming pattern. *Journal of Climate*, *29*(20), 7265–7279. https://doi.org/10.1175/JCLI-D-16-0039.1